Generally, the arithmetic mean temperature difference Δt_{am} is greater than the logarithmic mean temperature difference Δt_{lm}, so that the overall coefficient of heat transmission K_{am} is less than K_{lm}.

The recovery efficiency η_{rec} of the heat exchanger can be calculated by eq. (26), and the temperature efficiency Φ_g of the heat exchanger is defined as

$$\Phi_g=(t_{g1}-t_{g2})/(t_{g1}-t_{w1}). \tag{40}$$

The outlet gas temperature t_{g2} and outlet water temperature t_{w2} can be calculated by expressing the inlet gas temperature t_{g1} and the inlet water temperature t_{w1} as follows:

$$t_{g2}=t_{g1}-\Phi_g(t_{g1}-t_{w1}) \ \ {}^\circ\mathrm{C}, \tag{41}$$

$$t_{w2}=t_{w1}+(c_{pgm}G_g/c_wG_w)\Phi_g(t_{g1}-t_{w1}) \ \ {}^\circ\mathrm{C}. \tag{42}$$

The mean value of K_{lm}, η_{rec}, and Φ_g for ST-3 are obtained by experiment as shown in Table A-6 in Appendix.

$$K_{lm}=35.1 \ \mathrm{kcal/m^2h^\circ C}, \quad \eta_{rec}=0.715, \quad \text{and } \Phi_g=0.860.$$

(*b*) *Heating cpacity Q_{R2} obtained from measurement of inlet and outlet water temperatures*

The heat transferred from the hot exhaust gas to the water will also be estimated by

$$Q_{R2}=c_wG_w(t_{w2}-t_{w1})+\sum\alpha_aA_{wa}(t_{wm}-t_a) \ \ \mathrm{kcal/h}. \tag{43}$$

The last term of eq. (43) shows the heat loss from the hot surface area of the shell contacting water on its inner side and atmospheric air on its outer side by natural convection. The heating capacity obtained by this method occasionally entails some errors due to the difficulty of measuring the small temperature difference $(t_{w2}-t_{w1})$.

(*c*) *Heating capacity Q_{R3} obtained from measurement of water temperature rise in a bathtub as heating load*

A new method of obtaining the heating capacity of a heat exchanger was devised by AWANO, one of the authors. It depends on the measuring of mean water temperature rise of a bathtub with time. The principle is as follows:

For a small time interval $d\tau$, the following heat equilibrium equation should be valid:

$$\begin{aligned}(Q_{R3}+Q_p)d\tau&=[K_{am}F_i(t_{gm}-t)+Q_p]d\tau\\&=(c_wG_w+\sum c_MG_M)dt+\sum\alpha_aA(t-t_a)d\tau,\end{aligned} \tag{44}$$

where

Q_p: pump work supplied, kcal/h,
G_w: total weight of water contained in the bathtub, heat exchanger, pump, and pipe lines, kg,
t_0: initial temperature of water in the bathtub, °C,
t_{gm}: mean gas temperature, which is kept nearly constant but rises slightly with time, °C,
t: instantaneous mean temperature of water, °C,
$\sum c_M G_M$: total sum of heat capacities of materials to be heated by water, such as shell, tubes, piping, pump, and bathtub, kcal/°C,
A: cooling surface area of shell, piping, pump, and bathtub, which contact water on the inside and atmospheric air on the outside, m²,
τ: time, h.

From eq. (44), we get

$$\frac{dt}{d\tau}=a-bt, \tag{45}$$

where

$$a=(K_{am}F_i t_{gm}+\sum\alpha_a A t_a+Q_p)/(c_w G_w+\sum c_M G_M)\ \ {}^\circ\mathrm{C/h}, \tag{46}$$

$$b=(K_{am}F_i+\sum\alpha_a A)/(c_w G_w+\sum c_M G_M)\ \ 1/\mathrm{h}. \tag{47}$$

By integrating eq. (45), the instantaneous mean water temperature t in the bathtub can be represented by

$$t=(a/b)-[(a/b)-t_0]e^{-b\tau}\ \ {}^\circ\mathrm{C}. \tag{48}$$

For determining the constant term (a/b) in eq. (48), the following approximation is very useful. From eqs. (46) and (47), the constant term (a/b) can be estimated by neglecting the heat-loss terms $\sum\alpha_a A t_a$ and $\sum\alpha_a A$ and pump work Q_p as follows:

$$(a/b)\fallingdotseq K_{am}F_i t_{gm}/(K_{am}F_i)=t_{gm}\ \ {}^\circ\mathrm{C}, \tag{49}$$

and from eq. (48),

$$e^{-b\tau}=(t_{gm}-t)/(t_{gm}-t_0). \tag{50}$$

The mean value of b can be determined from eq. (50) by experiment, and the overall coefficient of heat transmission K_{am} can be determined from eq. (47) by

$$K_{am}=[b(c_w G_w+\sum c_M G_M)-\sum\alpha_a A]/F_i\fallingdotseq b(c_w G_w)/F_i\ \ \mathrm{kcal/m^2h^\circ C}. \tag{50}$$

As an example, the instantaneous water temperature in a bathtub in an experiment with ST-3 as shown in Table A-6 in Appendix can be represented as follows:

$$t_{gm}=207\,°\text{C}, \qquad t_0=31\,°\text{C},$$

$$t=t_{gm}-(t_{gm}-t_0)e^{-b\tau}=207-176e^{-0.406\tau}\ °\text{C}, \tag{51}$$

$$b=0.406\ 1/\text{h}, \quad c_w=1\ \text{kcal/kg}\,°\text{C}, \quad G_w=286.5\ \text{kg}, \quad F_i=6.02\ \text{m}^2.$$

From eq. (50), we get

$$K_{am}=b(c_wG_w)/F_i=0.406(1)(286.5)/6.02=19.3\ \text{kcal/m}^2\text{h}\,°\text{C}.$$

As a more accurate calculation,

$$c_MG_M=0.11(140)+0.11(169)+0.11(20)+0.33(8)+0.23(7.8)$$
$$=\underset{\text{(bathtub)}}{15.4}+\underset{\text{(shell and tube)}}{18.6}+\underset{\text{(pump)}}{2.2}+\underset{\text{(rubber hose)}}{2.6}+\underset{\text{(aluminum radiator)}}{1.8}=40.6\ \text{kcal/}°\text{C},$$

$$\sum\alpha_aA=4.8(1.48)+[5(0.443)+4(1.584)+2(0.433)]+5.5(0.834)$$
$$=\underset{\text{(shell side)}}{7.10}+\underbrace{[\underset{\text{(upper surface)}}{2.22}+\underset{\text{(sidewall)}}{6.34}+\underset{\text{(lower surface)}}{0.87}]}_{\text{[bathtub]}}+\underset{\text{(rubber hoses)}}{4.59}=21.1\ \text{kcal/h}\,°\text{C}.$$

Hence,

$$K_{am}=[b(c_wG_w+\sum c_MG_M)-\sum\alpha_aA]/F_i=[0.406(1)(286.5)+0.406(40.6)-21.1]/6.02$$
$$\doteq[116.3+16.5-21.1]/6.02=18.6\ \text{kcal/m}^2\text{h}\,°\text{C},$$

and the transferred heat

$$Q_{R3}=K_{am}F_i(t_{gm}-t)=18.6(6.02)(207-t)$$
$$=112(207-t)=23180-112t\ \text{kcal/h}. \tag{52}$$

(*d*) *Heating capacity Q_{R4} obtained by measuring the time necessary for completely melting an ice block floating on the water in a bathtub*

A most simple method for measuring the heating capacity of an exhaust-gas heat exchanger is obtained by measuring the time necessary to completely melt an ice block floating in the water in a bathtub and the temperature of water in the bathtub.

τ_m: time necessary for melting, h,
r: latent heat of fusion of ice, $r=80$ kcal/kg,
t_{B0}: initial temperature of water in the bathtub, °C,

c_I: specific heat of ice, kcal/kg°C,
t_{Bf}: final temperature of water in the bathtub, °C,
t_{Bm}: mean temperature of water, $t_{Bm}=(t_{B0}+t_{Bf})/2$, °C
t_a: atmospheric temperature, °C,
G_W: total weight of water contained in the water system, *i.e.*, heat exchanger, water piping, pump, and a bathtub, kg,
G_I: weight of ice block, kg,
t_I: initial temperature of ice, °C.

The equation of heat balance can be written as follows:

$$[Q_{R4}+Q_p+\sum\alpha_a A(t_a-t_{Bm})]\tau_m=G_I(-c_I t_I+r+c_w t_{Bf})+c_w G_w(t_{Bf}-t_{Bo}). \quad (53)$$

Hence, the transferred heat will be

$$Q_{R4}=K_{am}(t_{gm}-t_{Bm})F_i=[G_I(-c_I t_I+r+c_w t_{Bf})+c_w G_w(t_{Bf}-t_{Bo})]/\tau_m$$
$$-[Q_p+\sum\alpha_a A(t_a-t_{Bm})] \text{ kcal/h}. \quad (54)$$

The last term of eq. (54), which is pump work and the transferred heat from atmosphere to water, may be ignored as a first approximation, whereby the overall coefficient K_{am} can be calculated by

$$K_{am}=[G_I(-c_I t_I+r+c_w t_{Bf})+c_w G_w(t_{Bf}-t_{B0})]/[\tau_m(t_{gm}-t_{Bm})F_i] \text{ kcal/m}^2\text{h°C}. \quad (55)$$

As an example, in Table A-5 in Appendix 3 for the heat exchanger ST-2,

$$G_w=257\text{ kg},\quad G_I=42.8\text{ kg},\quad t_I=0°\text{C},$$
$$t_{B0}=20°\text{C},\quad t_{Bf}=20°\text{C},\quad t_a=18°\text{C},$$
$$\tau_m=0.2388\text{ h},\quad t_{g1}=300°\text{C},\quad t_{g2}=39°\text{C},$$
$$t_{gm}=170°\text{C},\quad t_{Bm}=20°\text{C},\quad F_i=6.47\text{ m}^2.$$

From eq. (55),

$$K_{am}=[42.8(80+1\times20)+(1)(257)(20-20)]/[0.2388(170-20)(6.47)]$$
$$=[4280+0]/[0.2388(150)(6.47)]=18.5\text{ kcal/m}^2\text{h°C},$$

$$Q_{R4}=K_{am}F_i(t_{gm}-t)=(18.5)(6.47)(170-t)$$
$$=119.7(170-t)=20350-120t\text{ kcal/h}. \quad (56)$$

In eq. (56), t denotes the hot-water temperature in the bathtub at any time τ.

In Appendix 2, the theoretical calculations on the design of a shell-and-tube type exhaust-gas heat exchanger ST-3 are explained.

In Appendix 3, the experimental data on the exhaust-gas heat exchangers, such as shell-and-coil type, shell-and-tube type, and vertical fin-tube type, are described.

8. Bubble Type Exhaust-Gas Heat Exchanger

8.1. Two-stage bubble type heat exchanger for making hot water and melting ice

As a result of many experiences during the last twenty years on the exhaust-gas heat exchangers for recovering exhaust-gas energy from diesel engines, the following two difficulties were recognized:

(a) Acid corrosion of heating surfaces

(b) Decrease of heat transfer with time due to the soot fouling of heating surfaces.

To overcome these difficulties, the authors developed a new bubble type exhaust-gas heat exchanger for JARE-18 (1976/78). In this heat exchanger, the engine exhaust gas is blown into the bottom of a body of water in a heating tank through many small holes. As the bubbles rise through the water, the heat of the bubbles is transferred to the surrounding water through the bubble surfaces. In other words, the bubble surface itself makes the heating surface, and the temperature of the bubble surface will be nearly equal to the water temperature because the heat transfer coefficient of water boundary layer is very great. Accordingly, the heat transfer from each bubble to water depends mainly on thermal conduction in the bubble. The necessary minimum depth of water required for fully transferring the heat in a bubble to the water decreases with decreasing diameter of the bubble.

In Figs. 45 and 46, a diagrammatic sectional view of the new heat exchanger and its external view are shown. In Fig. 45, the engine exhaust flows down through a center tube surrounded by a water jacket and is blown into the water of the lower heating tank through three perforated plates. The delivery gas from the lower heating tank is led to the surrounding space of an upper heating tank and is blown again into the water of the upper heating tank where its remaining heat is transferred to the water.

The gas from the upper heating tank is exhausted into the air through three collecting pipes and a flexible tube connecting them to a chimney. The cold water is fed to a float chamber in order to keep a constant water level H_U in the upper heating tank. To the side of the lower heating tank, a hot-water reservoir tank was installed, in which a pair of electrodes for detecting the water level H_L

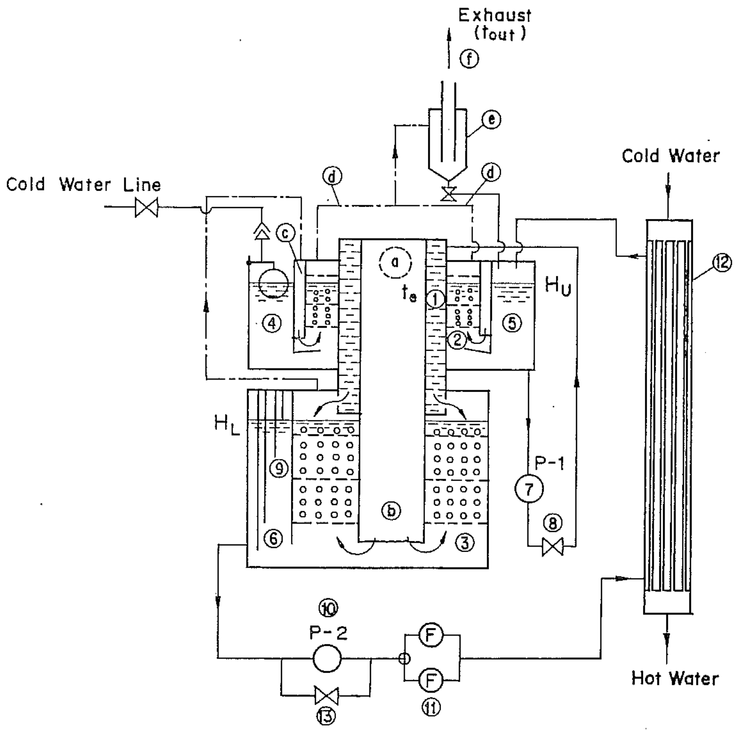

Fig. 45. Bubble type exhaust-gas heat exchanger BE-1 prepared for JARE-18 (1976/78).

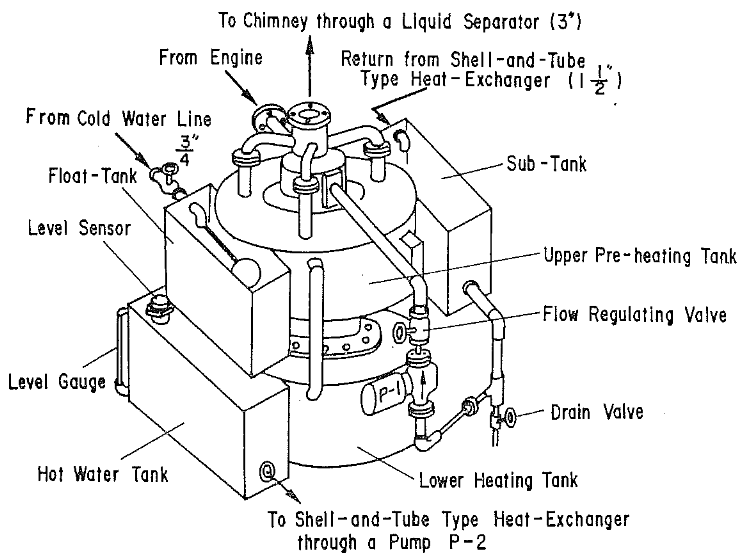

Fig. 46. Bubble type exhaust-gas heat exchanger BE-1 prepared for JARE-18.

When the bubbles of the engine exhaust rise up through the water in the heating tank, the bubble gases will be saturated by steam having a partial pressure p_s corresponding to the water temperature through which the bubbles finally rise. The saturated steam G_{ws} can be calculated by eqs. (18) and (19), and the total gas flow G_{out} can be obtained by eq. (21).

If the outlet gas temperature t_{out} is low, some of the water vapor contained in the engine exhaust G_w will be condensed as the gas flows through the water, and the condensed water vapor G_{wc} can be calculated by eqs. (22) or (23). On the contrary, however, if the temperature t_{out} is higher than about 32–38°C, some part of the water in the heating tank will evaporate until the partial pressure of water vapor reaches p_s corresponding to water temperature of the upper tank. In this case, the evaporated water in the heating tank can be estimated by

$$G_{we}=G_{ws}-G_w=G_{ws}-(G_{aw}+G_{gw})\ \text{kg/h}, \tag{57}$$

and the outlet heat from the chimney can be calculated by

$$Q_{\text{out}}=(h_{gd})_{\text{out}}G_{gd}+(h'')G_{ws}\ \text{kcal/h}. \tag{58}$$

The available maximum energy, Q_A recovered from the energy of the engine exhaust $Q_e=H_{g1}$ calculated by eq. (14) becomes

$$Q_A=Q_e-Q_{\text{out}}\ \text{kcal/h} \tag{59}$$

$$=Q_B+Q_H+Q_{\text{Loss}}\ \text{kcal/h}, \tag{60}$$

where

Q_B: heat absorbed by hot-water tank, bathtub, or ice-melting tank,
Q_H: heat required for heating the water contained in the heating tank, pipelines, and radiator,
Q_{Loss}: heat loss from heating tank, pipelines, and bathtub.

The maximum recovery efficiency of the heat exchanger is

$$(\eta_{\text{rec}})_{\max}=Q_A/Q_e. \tag{61}$$

Two experiments on the new bubble type exhaust-gas heat exchanger were conducted by the authors in the Engine Laboratory of Nihon University, Tokyo.

Figs. 48 and 49 show the flow diagrams of water for No. 1 and No. 2 experiments respectively. In No. 1 experiment, the upper heating tank (HU) and the lower heating tank (HL) of the heat exchanger were connected in series. A recirculating water pump P-2 with a flow rate of 6840 kg/h fed the hot water of the heat exchanger to a radiator submerged in a bathtub containing 200 kg of water. The rise of the water temperature in the bathtub was measured and was

$$a/b = (K_R F_R t_{Rm} + \sum \alpha_a A t_a)/(K_R F_R + \sum \alpha_a A) \doteqdot t_{Rm}, \quad (65)$$

K_R: overall coefficient of heat transmission of radiator, kcal/m²h°C,
F_R: heating surface area of radiator, m²,
t_{Rm}: mean water temperature in radiator, °C,
G_B: weight of water in the bathtub, $G_B = 200$ kg,
c_w: specific heat of water, 1 kcal/kg°C.

The other notations are the same as in eq. (44).

For No. 1 experiment,

$$t_B = t_{Rm} - (t_{Rm} - t_{B0}) e^{-b\tau} = 79 - (79 - 11.5) e^{-0.98\tau} \ \text{°C}. \quad (66)$$

From eq. (64),

$$K_R F_R \doteqdot b\, c_w G_B = (0.98)(1)(200) = 196 \ \text{kcal/h°C},$$

so that

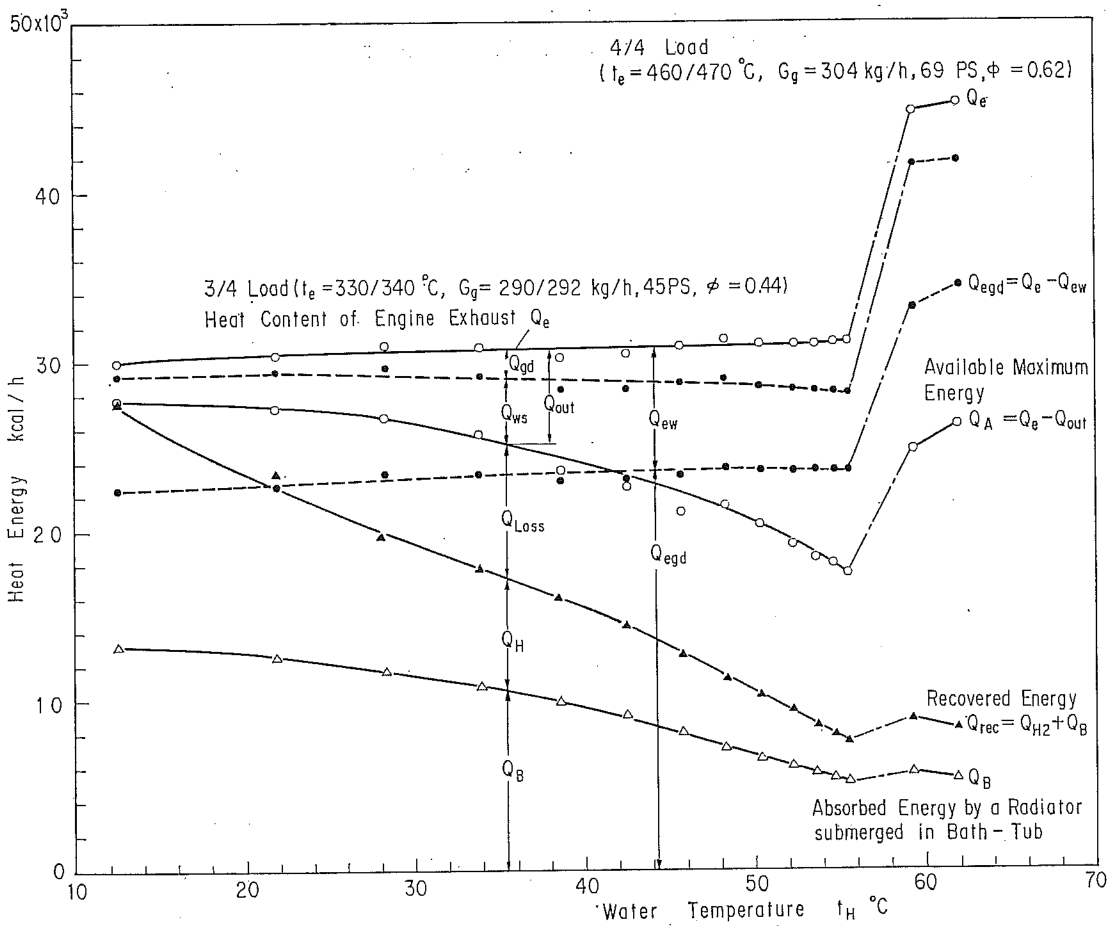

Fig. 50. Results of experiment No. 1 on a BE-1 bubble type exhaust-gas heat exchanger.

$$Q_B = K_R F_R (t_{Rm} - t_B) = 196(79 - t_B) = 15480 - 196 t_B \text{ kcal/h.} \quad (67)$$

In the same way, from the measured temperature of water in the heating tank t_H, which is heated by bubble gas with temperature t_{Hb} and the heating surface area F_{Hb}

$$t_H = t_{Hb} - (t_{Hb} - t_{H0}) e^{-b\tau} = 59.5 - (59.5 - 12.6) e^{-2.30\tau} \ {}^\circ\text{C}, \quad (68)$$

$$K_{Hb} F_{Hb} \doteqdot b\, c_w G_H = (2.30)(1)(118) = 271 \text{ kcal/h}^\circ\text{C},$$

$$Q_H = K_{Hb} F_{Hb} (t_{Hb} - t_H) = 271(59.5 - t_H) = 16125 - 271 t_H \text{ kcal/h,} \quad (69)$$

where G_H is the weight of the water contained in the heating tank ($G_H = 118$ kg) and its initial temperature $t_{H0} = 12.6^\circ$C. The maximum recovery efficiency $(\eta_{rec})_{max}$ is 0.923–0.562 for this system and 27600–17500 kcal/h can be recovered by this system. The results of No. 1 experiment are shown in Fig. 50.

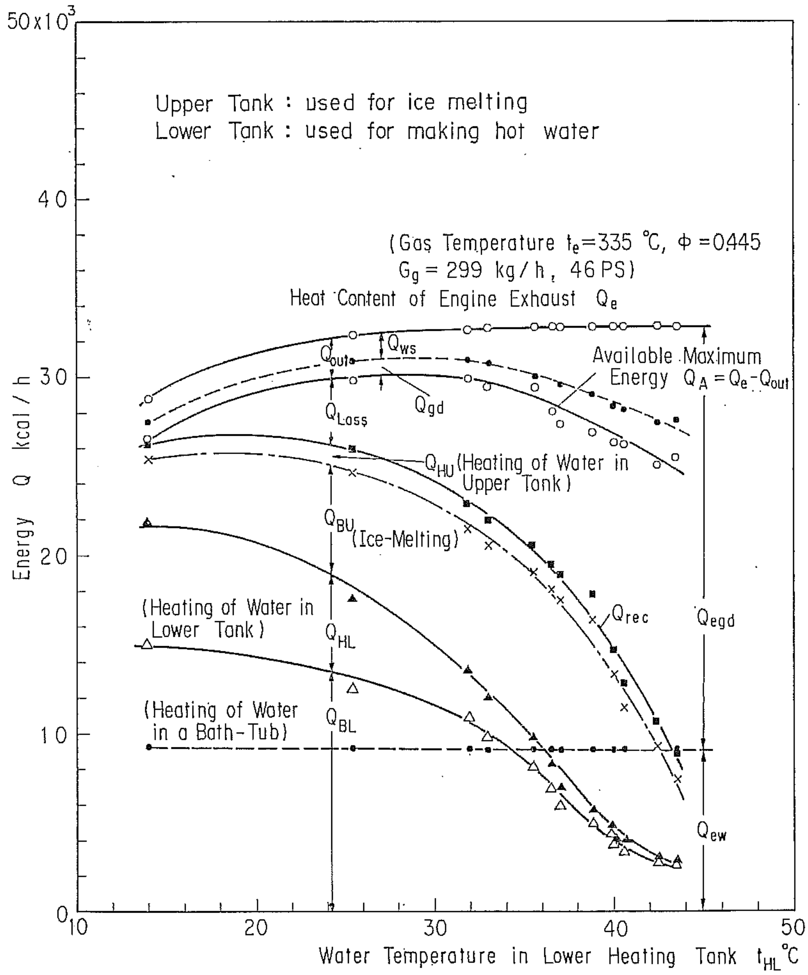

Fig. 51. Results of experiment No. 2 on a BE-1 bubble type exhaust-gas heat exchanger.

9. Heat Exchangers for Recovering Coolant Heat of Diesel Engines

9.1. Horizontal shell-and-tube type heat exchangers

For JARE-7 (1965/67), the authors developed a horizontal shell-and-tube type heat exchanger for recovering coolant waste heat from diesel engines driving 45-kVA electric generators. General views are shown in Fig. 52, and the design data are given in Table 11. Two sets of the coolant-to-water heat exchangers

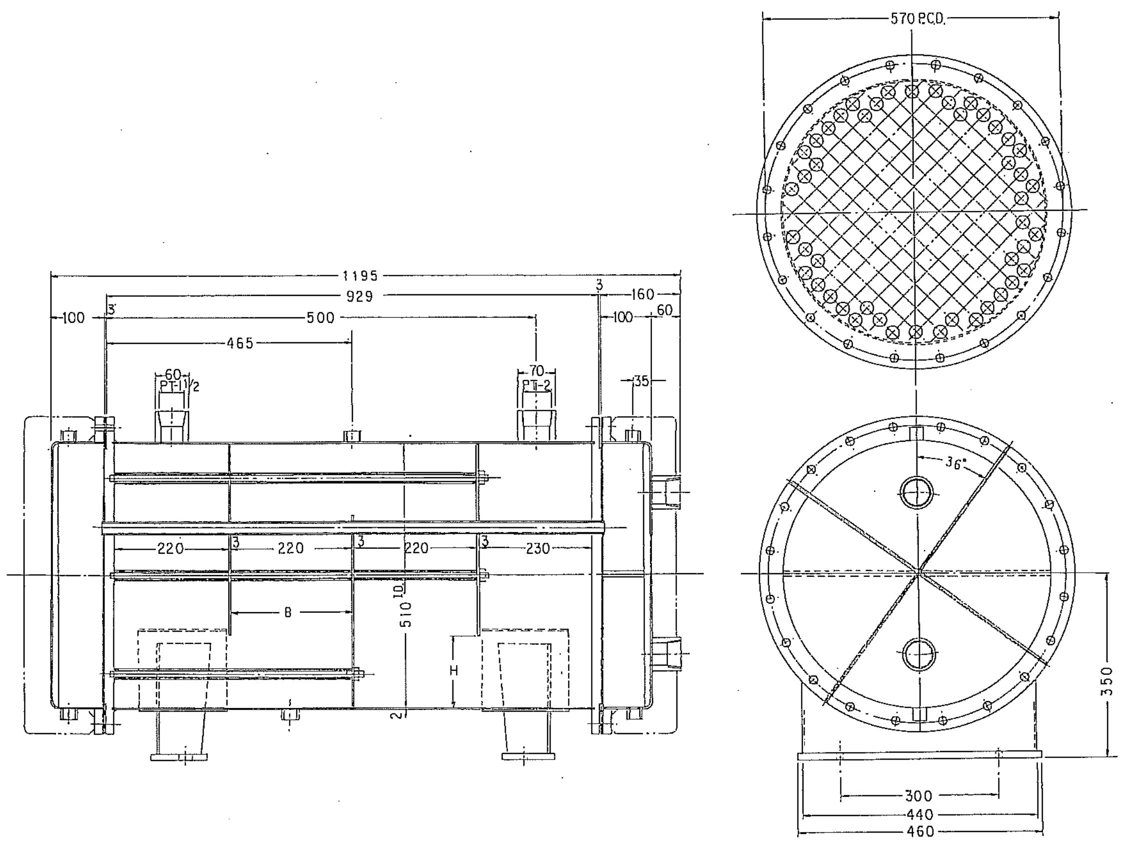

Fig. 52. Horizontal shell-and-tube type heat exchanger prepared for JARE-7 (1965/67) to recover coolant heat of diesel engine.

Table 11. Shell-and-tube type coolant heat recovery heat exchangers and secondary heat exchanger prepared for JARE.

Items	JARE-7 (1965/67)	JARE-10 (1968/70)	JARE-13 (1971/73)- JARE-20 (1978/80)
Capacity Q_c (kcal/h)	50000	60000	45000
Type	horizontal	horizontal	vertical
Purpose	coolant heat recovery (45 kVA)	coolant heat recovery (65 kVA)	secondary heat exchanger
Shell side			
Shell			
Material	SUS-28	SUS-32	SUS-28TPA
Outer diam. (mm)	515	506	165.2 (6B)
Inner diam. (mm)	510	500	158.4
Total length (mm)	1255	1836	1179
Center height (mm)	350	350	—
Liquid (t_{o1}, t_{o2} °C)	coolant (80, 74)	cold water (65, 70)	cold water (12, 16)
Tube plate			
Material	SUS-28	SUS-32	SUS-28
Outer diam. (mm)	610	655	265
Thickness (mm)	18	22	22
Pipe arrangement	square	triangle	triangle
Pitch P_t (mm)	32	34	23
Number of tubes Z	164	146	26
Baffle plate			
Number N	3	7	5
Thickness	3	3	3
Distance	220×3+230	179×7+176	160×5+173
Equivalent diam. of tube space D_e (mm)	27.2	26	14.4
Effective flow area a_s (m^2)	0.02482	0.02396	0.00539
Flow rate (l/min)	160	200	200
(kg/h)	9600	12000	12000
Flow velocity w_o (m/s)	0.1035	0.1426	0.618
Reynolds number R_e	7163	8897	7119
Baffle-cut ratio A/D_s	0.278	0.263	0.242
Nusselt number Nu	58.1	69.5	95.8
Heat transfer coefficient α_o (kcal/m^{2}h°C)	1227	1526	3380
Temperature efficiency Φ_o	0.404	0.328	0.0556
Pipe diameter	2B	2B	1B
Tube side			
Material	SUS-28TPS	SUS-32TPS	SUS-28TB
Outer diam. d_o (mm)	25	25	18

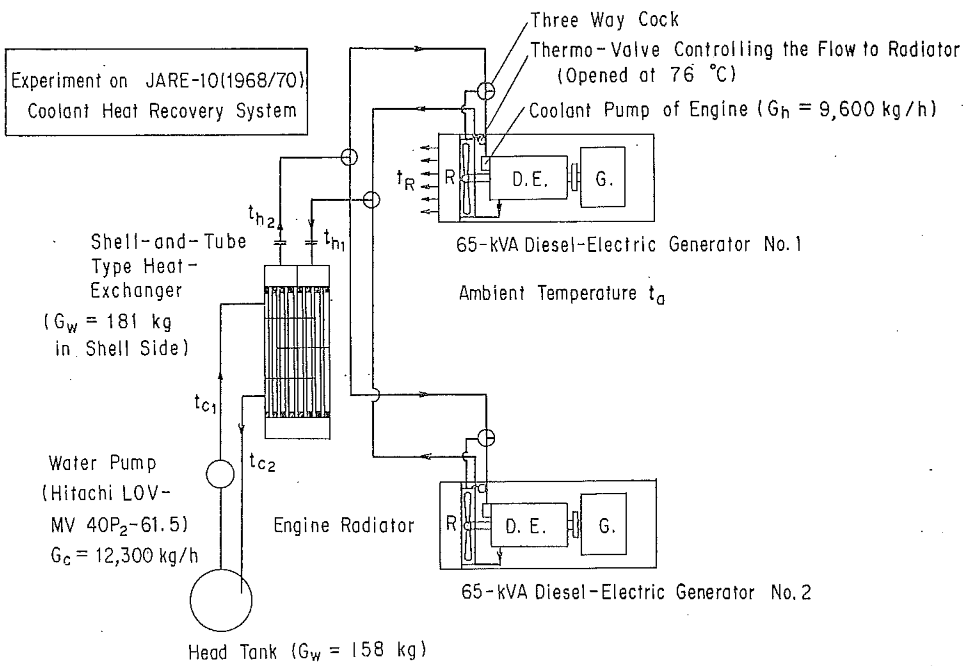

Fig. 54. Experiment on the horizontal shell-and-tube type heat exchanger prepared for JARE-10 (1968/70) to recover coolant heat of diesel engine. Experiment was carried out at Nakajima Denki Co., Ltd. in November 1968. The results are shown in Table 12.

JARE-7 engine room. The hot water was fed to the living quarters and to a bathtub.

For JARE-10 (1968/70), the same type horizontal heat exchanger, but with slightly larger heating capacity, was manufactured and installed in the JARE-9 engine room and was used for absorbing the coolant heat of a diesel engine driving a 65-kVA electric generator (Figs. 53, 54; Table 12). The hot water was stored in another hot-water tank installed in the JARE-9 engine room and used for room-heating in the living quarters of the JARE-9 engine room (Fig. 16).

For JARE-19 (1977/79), engine power was increased for driving the 110-kVA electric generator, and the waste heat recovering system was also rearranged from that shown in Fig. 16 to that in Fig. 18.

The engine coolant of the 110-kVA engine was recirculated through a headtank installed near the engine, and the coolant in the headtank was fed to a horizontal heat exchanger installed in the JARE-7 engine room, which was separated from the JARE-9 engine room by about 40 m, and also to a radiator submerged in a 10 k*l* snow melting tank installed outdoors and returned again to the headtank. The hot water heated by the horizontal heat exchanger was stored in the hot-water tank of the JARE-7 engine room and supplied to a bathtub and the living quarters.

Another horizontal heat exchanger was used as a secondary heat exchanger in

the exhaust energy recovering system as shown in Fig. 18. For preventing severe corrosion of exhaust-gas heat exchangers, the water temperature should be kept as high as possible. For this purpose, the horizontal heat exchanger was used as a secondary heat exchanger. In the secondary water-to-water heat exchanger, the heat recovered from the exhaust gas was transferred again to the secondary hot water with a lower temperature than the primary water. The secondary hot water was supplied to eight radiators for room-heating in the living quarters of the JARE-9 engine room. A fan-coil unit radiated 4500 kcal/h of heat. During JARE-20 (1978/80), the waste heat recovery system was rearranged again from that shown in Fig. 18 to that in Fig. 19. In this system, the horizontal heat exchanger, which had been used as a secondary heat exchanger in the exhaust-gas energy recovering system was removed because the hot-water tank in the JARE-9 engine room could supply hot water directly to the exhaust-gas heat exchanger, but the horizontal coolant-to-water heat exchanger in the coolant-heat recovery system has been retained until now.

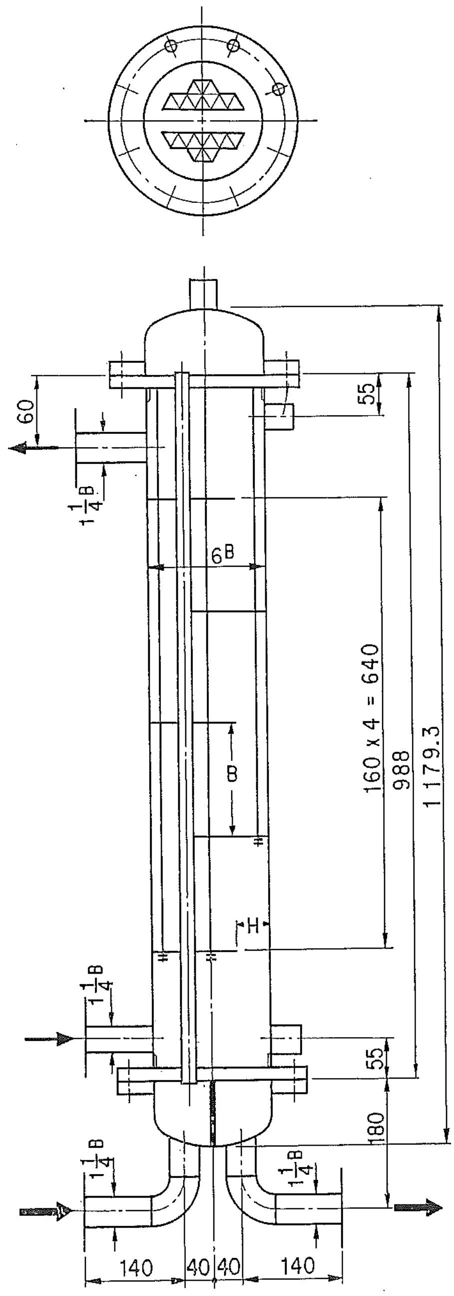

Fig. 55. Vertical shell-and-tube type heat exchanger prepared for JARE-13 (1971/73) as the secondary water-to-water heat exchanger to recover exhaust-gas energy of diesel engine.

9.2. Vertical shell-and-tube type water-to-water secondary heat exchanger

For two reasons, the first to protect the heating surface of exhaust-gas heat exchangers from acid corrosion, and the second to remove the radiators submerged in the 130-k*l* outdoor cold-water reservoir tank and in the 10-k*l* snow-melting tank, a small vertical shell-and-tube type heat exchanger as shown in Fig. 55 was developed by the authors for JARE-13 (1971/73).

Hot water receives heat during its flow through the coil of an exhaust-gas heat exchanger and is led to the inside of tubes of a vertical water-to-water heat exchanger to warm the cold water of shell side, which recirculates to outdoor water tanks.

This process has been used effectively since JARE-13 up to the present to keep the water in outdoor tanks from freezing.

9.3. Estimation of thermal performance of a shell-and-tube heat exchanger

Thermal performance can be estimated by the following method:

Symbols;

Q_c: recoverd coolant heat, kcal/h,
t: temperature of water, °C,
G: flow rate of water, kg/h,
F_o: total outer heating area, m^2,
d: diameter of tubes, m,
z: total number of tubes,
l: length of a tube, m,
A_i: total inner sectional area of tubes, m^2,
D_s: inner diameter of shell, m,
N: number of baffle plates,
H: height of baffle cut, m,
B: distance between to baffle plates, m,
D_e: equivalent diameter for flow at the outside of tubes, m,
α: heat transfer coefficient, kcal/m²h°C,
K_o: overall coefficient of heat transmission, kcal/m²h°C,
Δt_{lm}: logarithmic mean temperature difference, °C,
V: volume flow rate, m³/s,
a_s: area of minimum flow among three tubes (triangle arrangement) or four tubes (square arrangement), m^2,
δ_M: thickness of tube wall, m,
λ_M: thermal conductivity of tube material, kcal/mh°C,
Φ: temperature efficiency,
w: velocity, m/s,
ν: kinematic viscosity, m²/s,
R_e: Reynolds number, $R_e = wD_e/\nu$,
P_r: Prandtl number,
Nu: Nusselt number, $Nu = \alpha D_e/\lambda$,
λ: thermal conductivity of water, kcal/mh°C,
c: specific heat of water, kcal/kg°C

Subscripts;

i: inside of tubes, o: outside of tubes,
1: inlet, 2: outlet.

In a steady state, the following equations of heat balance should be satisfied:

$$Q_c = c_i G_i (t_{i1} - t_{i2}) = c_o G_o (t_{o2} - t_{o1}) \text{ kcal/h}, \tag{70}$$

$$\Phi_i = (t_{i1} - t_{i2})/(t_{i1} - t_{o1}), \tag{71}$$

$$\Phi_o = (t_{o2} - t_{o1})/(t_{i1} - t_{o1}). \tag{72}$$

Substituting eqs. (71) and (72) into (70), we get (JSME, 1966)

$$Q_c = c_i G_i \Phi_i (t_{i1} - t_{o1}) = c_o G_o \Phi_o (t_{i1} - t_{o1}) \text{ kcal/h}. \tag{73}$$

The heat transfer coefficient of water flowing through the tubes is given by

$$(Nu)_i = 0.023 (R_e)_i^{0.8} (Pr)_i^{0.4} = \alpha_i d_i / \lambda_i, \tag{74}$$

and the heat transfer coefficient of flow outside of the tubes can be estimated by LYDERSEN (1979)

$$(Nu)_o = 0.224 (R_e)_o^{0.587} (H/D_s)^{-0.4} (Pr)_o^{1/3} = \alpha_o D_e / \lambda_o. \tag{75}$$

In this equation, the equivalent diameter D_e for the flow across the tube bank can be represented by

(for triangle arrangement with pitch P_t)

$$D_e = [2\sqrt{3} P_t^2 / (\pi d_o)] - d_o \text{ m}, \tag{76}$$

and

(for square arrangement with pitch P_t)

$$D_e = [4 P_t^2 / (\pi d_o)] - d_o \text{ m}. \tag{77}$$

The velocity w_e past the tube bank in, or closest to, the center is

$$w_o = V_o / a_s \text{ m/s}, \tag{78}$$

where

$$a_s = (D_s / P_t)(P_t - d_o) B \text{ m}^2, \tag{79}$$

which is the minimum area between two tubes of a flow passage.

The Reynolds number of flow at the outside of tubes is calculated by

$$(R_e)_o = w_o D_e / \nu_o. \tag{80}$$